2000

Ambiguity Function of an Ultrawideband Random Noise Radar

Muhammad Dawood
University of Nebraska-Lincoln

Ram M. Narayanan
University of Nebraska-Lincoln

Published in IEEE Antennas and Propagation Society International Symposium, 2000. Vol. 4, pp. 2142-2145; doi: 10.1109/APS.2000.874917

Ambiguity Function of an Ultrawideband Random Noise Radar

Muhammad Dawood* and Ram M. Narayanan
Department of Electrical Engineering and Center for Electro-Optics
University of Nebraska, Lincoln, NE 68588-0511
Tel: 402-472-5141, Fax: 402-472-4732, Email: rnarayanan@unl.edu

1 Introduction

The University of Nebraska has developed an ultra-wideband (UWB) random noise radar system which transmits an ultra-wideband random noise (Gaussian) waveform with a uniform power spectral density (PSD) in the 1-2 GHz frequency range. The ability of the system to characterize the Doppler shift of moving targets exhibiting varying linear and rotational velocities was clearly demonstrated [1, 2].

In this paper, we look at the range and range rate resolution issues by analyzing the Woodward's ambiguity function [3]. In general, the radar signal ambiguity function is defined as the normalized response of a filter matched to a return signal with range rate V_o, to a return signal with range rate V_1. It describes the resolution properties of a given signal in range and range rate. However, for a random noise radar a correlator matched to transmit process is required. Therefore, an analogous ambiguity function may be defined as the expected value of the response of the correlator matched to a target moving with range rate V_o, to the return signal from the target with range rate V_1. Moreover, for a UWB transmit random process, the compression or stretch due to the range rate on the envelope of the return process cannot be ignored.

2 Radar System Description

A simplified block diagram of the random noise radar system is shown in Fig. 1. The noise source produces a signal with a Gaussian amplitude distribution, constant PSD, in the 1-2 GHz frequency range. One of the noise source output, after being split in power divider PD1, is amplified in a broadband power amplifier AMP1 and transmitted. The second output of PD1 is connected to a combination of a fiber optic (FO) fixed delay line DL1 and a digitally controlled variable delay line DL2. The fixed delay line is used to set the minimum range to the target and provides a delay of 1.5 μs with 0 dB insertion loss, while the variable delay line can be programmed for delays from 0 to 19.968 ns in 0.156 ns steps. The delay line output is mixed with the output of a 160 MHz phase-locked oscillator OSC2 in a lower sideband up-converter MXR1. The up-converter output, in the 0.84-1.84 GHz frequency range, feeds MXR2. The 1-2 GHz received signal provides the second input to mixer MXR2. Thus, the output of mixer MXR2 is always at 160 MHz, since the two mixer inputs are shifted by 160 MHz. The 160 MHz output of MXR2 is filtered in a 160 MHz bandpass filter (BPF) and is fed to the I/Q detector. The 160 MHz oscillator OSC2 also feeds the I/Q detector. Thus, the I/Q detector yields the in-phase (I) and quadrature (Q) components of the received signal.

3 Theoretical Considerations

The transmit waveform of the system can be modeled as a Gaussian band pass process centered at some frequency ω_o for $\omega_o > B/2$, i.e.,

$$X(t) = X_c(t)cos\,(\omega_o t) - X_s(t)sin\,(\omega_o t) \tag{1}$$

in terms of uncorrelated (i.e. $E[X_c X_s] = 0$]) low frequency zero means Gaussian in-phase I and quadrature Q components with variance $E[X_c^2] = E[X_s^2]$.

803-6369-8/00/$10.00 ©2000 IEEE

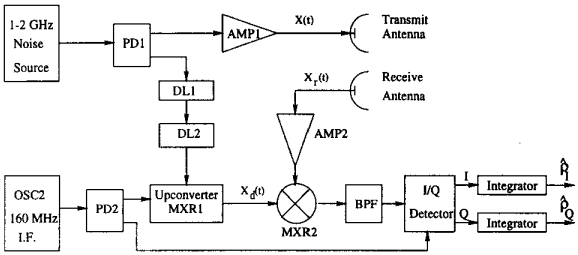

Figure 1: Block diagram of ultra-wideband random noise radar.

We assume a point target with constant range rate of $R = R_o + V_o t$, with resulting delay $\tau_o = 2R_0/(c + V_o) \simeq 2R_0/c$, and delay rate $\alpha = \frac{2V_o}{c-V_o} \simeq \frac{2V_o}{c}$. The received signal at the radar in response to the above transmitted signal can be

$$X_r(t) = k_1 \{V_1(\alpha, t, \tau_o) cos[\omega_o(1+\alpha)t - \omega_o\tau_o] - V_2(\alpha, t, \tau_o) sin[\omega_o(1+\alpha)t - \omega_o\tau_o]\} \quad (2)$$

where $V_1(.) = X_c[(1+\alpha)t - \tau_o]$, $V_2(.) = X_s[(1+\alpha)t - \tau_o]$, and k_1 is the arbitrary amplitude constant.

The output of the up-converter MXR1 can be written as

$$X_d(t) = k_2 \{X_c(t-\tau_d) cos[(\omega_o - \omega_{IF})t - \omega_o\tau_d] - X_s(t-\tau_d) sin[(\omega_o - \omega_{IF})t - \omega_o\tau_d]\} \quad (3)$$

where τ_d is the delay provided by delay lines and k_2 is an arbitrary amplitude constant.

The expected value of the estimated in-phase and quadrature cross-correlation components, $\langle\hat{\rho}_I\rangle$ and $\langle\hat{\rho}_Q\rangle$, can be shown to be

$$\langle\hat{\rho}_I(\alpha, \tau, t)\rangle = k_3 \int_{t-T}^{t} R_c(\alpha\lambda + \tau) cos(\alpha\omega_0\lambda + \omega_o\tau) h(t-\lambda) d\lambda \quad (4)$$

$$\langle\hat{\rho}_Q(\alpha, \tau, t)\rangle = -k_4 \int_{t-T}^{t} R_c(\alpha\lambda + \tau) sin(\alpha\omega_0\lambda + \omega_o\tau) h(t-\lambda) d\lambda \quad (5)$$

where $R_c(.) = sinc(.)$, $\tau = \tau_d - \tau_o$, $h(t)$ is the impulse response of the integrating filter, and T is the integration time. Furthermore, for optimum SNR, the integrating filter may be a bandpass filter of the form

$$h(t) = h_o(t) cos(\omega_d t) \quad (6)$$

where ω_d is the Doppler frequency of the target. Thus, a bank of filters centered at different frequencies can be used to extract the Doppler frequency due to the motion of the target.

The normalized average ambiguity function, $\langle\chi(\alpha, \tau, t)\rangle$, will be the rms sum (or envelope) of $\langle\hat{\rho}_I\rangle$ and $\langle\hat{\rho}_Q\rangle$, given by:

$$\langle\chi(\alpha, \tau, t)\rangle = \left| \int_{o}^{T} R_c(\alpha\lambda + \tau) h(t-\lambda) e^{-j\omega_o\alpha\lambda} d\lambda \right| \quad (7)$$

Eqn. 7 exactly describes the behavior of the radar correlator in time for all values of range and range rate. At this point, a useful check can also be made by assuming a narrow-band

process and ignoring the target motion effect on the envelope. This will make the integral in eqn. 7 operate on the filter alone. This result is similar to ref. [4] which highlights a desirable property of a narrow-band random process, i.e., the ambiguity function can be separated into range and range rate resolution functions which can be controlled independently. However, due to the ultra-wideband nature of the transmit process, range and range rate functions cannot be separated.

Since eqn. 7 is dependent on time also, its interpretation is slightly more complicated. One way to see the behavior of eqn. 7 may be to integrate it over time and then plot the resulting average ambiguity function in range and range rate. Figures 2 and 3 show this plot for different values of α, τ, and integration time T with filter bandwidth of 20 Hz. In general, we can observe that for $|\alpha| \neq 0$, the main lobe shifts from $\alpha = 0$ position, while its peak reduces and width increases, as is seen in Figure 2(b) and 3(b). Furthermore, for small integration time, the amplitude of the main peak is also reduced and the number of side lobes increase (Figure 3). Figure 2(c) shows slices of $\langle \chi(\alpha, \tau) \rangle$ in Doppler for different values of τ with integration time of 100 m sec; for $|\alpha| \neq 0$, the behavior similar to that discussed above is seen. A similar behavior is also seen for smaller integration time.

Figure 4 is the plot of $\langle \chi(\alpha, \tau, t) \rangle$ for $\tau = 0$ vs. time. As $|\alpha|$ increases, the main peak shrinks in height, its width in time decreases and side-lobes start appearing.

4 Conclusions

The wideband ambiguity function formulation demonstrates that given a sufficient integration time, two targets moving with different range rates may be resolved in range; however, the Doppler resolution seems poor. It also demonstrates the fact that although the Doppler resolution is primarily determined by the width of the Doppler filter, the integration time must be sufficient long to resolve two targets moving at slightly different velocities.

Acknowledgments

This work was supported by Office of Naval Research (ONR) contract # N00014-97-1-0200. We appreciate the helpful comments provided by Dr. William Miceli of ONR.

References

[1] Narayanan, R. M., Dawood, M., Mueller, R. D., and Palmer, R. D. (1997)
Doppler estimation using a coherent ultra-wideband random noise radar.
In *Proc. SPIE Conference on Radar Processing, Technology, and Applications*, Volume 3161, San Diego, CA, (August 1997), 70-76.

[2] Dawood, M., and Narayanan, R. M. (1999)
Doppler measurement using a coherent ultra-wideband random noise radar.
In *IEEE Antennas and Propagation Society International Symposium*, 1999 digest, Vol. 4, (July 1999), 2226-2229.

[3] Woodward, P.M. (1955)
Probability and Information theory with Applications to Radar.
McGraw Hill Book Company, 1955.

[4] Cooper, G. R., and Gassner, R. L., (1966)
Analysis of a wideband random signal radar system.
TR-EE66-9, Purdue University, Lafayette, Indiana, August 1966.

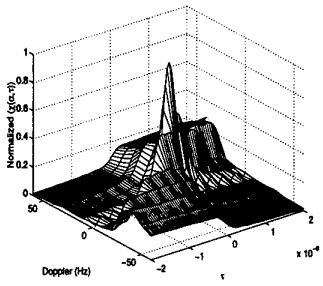

(a) Average ambiguity function $\langle\chi(\alpha,\tau)\rangle$

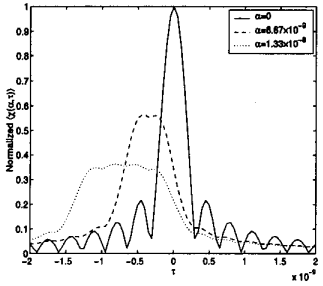

(b) Slice of $\langle\chi(\alpha,\tau)\rangle$ in delay τ

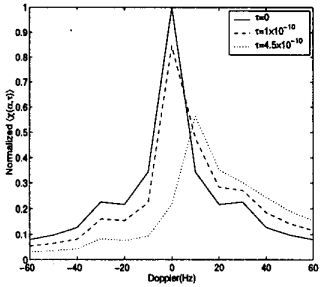

(c) Slice of $\langle\chi(\alpha,\tau)\rangle$ in Doppler

Figure 2: Normalized ambiguity function for an integration time of 100 m sec.

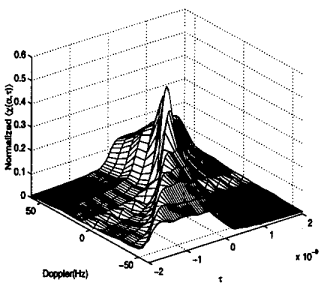

(a) Average ambiguity function $\langle\chi(\alpha,\tau)\rangle$

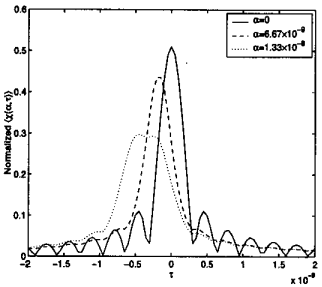

(b) Slice of $\langle\chi(\alpha,\tau)\rangle$ in delay τ

Figure 3: Normalized ambiguity function for an integration time of 50 m sec.

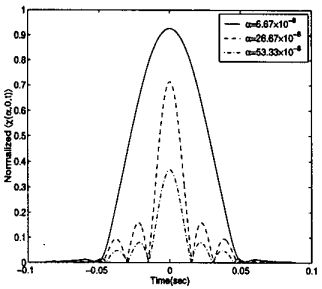

Figure 4: $\langle\chi(\alpha,0,t)\rangle$ for different α.